Proceedings 10th NUMGE 2023
10th European Conference on Numerical Methods in Geotechnical Engineering
Zdravkovic L, Kontoe S, Taborda DMG, Tsiampousi A (eds)

https://doi.org/10.53243/NUMGE2023-63

Simulated site amplification models for central and eastern North America using deep learning technique

O. Ilhan[1], Y. M. A. Hashash[2]

[1] *Department of Civil Eng., Ankara Yildirim Beyazit University, Ankara, Turkey*
[2] *Department of Civil and Environmental Eng., University of Illinois at Urbana-Champaign, Urbana, IL*

ABSTRACT: This paper presents a suite of deep learning/Artificial Neural Network (ANN)-based response spectrum (RS) site amplification models for Central and Eastern North America trained through large-scale one-dimensional (1D) site response simulations. ANNs significantly reduce the standard deviation of the residuals of simulated amplification estimations at CENA relative to conventional functions regressed using the identical amplification database. These observations indicate the inherent limitations of traditional relationships fitting a priori functional forms to simulated data as opposed to ANNs learning the actual behaviour of the dataset. To lend credence that ANNs might be an alternative to conventional models, the ANNs' performance in capturing site-specific responses is evaluated in this study. This evaluation shows that ANNs can account for the features of site-specific amplification (e.g., the amplitude and location of peak amplification) and can better reproduce the period elongation behaviour observed in nonlinear analyses as compared to their traditional counterparts.

Keywords: Site effects; site amplification; deep learning; artificial neural network; Central and Eastern North America

1 INTRODUCTION

The shallow soil layers are proven to alter the characteristics (i.e., amplitude, frequency content and duration) of the strong ground motion data (e.g., Seed et al., 1988;), and therefore site factors (e.g., BSSC, 2015) or site amplification models (e.g., Seyhan and Stewart, 2014) are incorporated into the seismic hazard calculations to account for the site effects. Site amplification models are developed to estimate the ground motion intensity measure (GMIM) at ground surface through the modification of GMIMs computed using ground motion models relative to reference site conditions (commonly taken as shear wave velocity (V_S) of 760 m/s and 3000 m/s for active (Frankel et al., 1996) and stable (Hashash et al., 2014) continental regions, respectively). The amplification functions based on the observed ground motions are scarce for Central Eastern North America (CENA) that is a stable continental region as compared to seismically active Western North America (WNA). The Next Generation Attenuation - East Geotechnical Working Group (NGA East - GWG) proposed empirical (Parker et al., 2019) and simulated (Harmon et al., 2019a, b, denoted as HEA19) response spectrum (RS) site amplification models, which were implemented (Stewart et al., 2020; Hashash et al., 2020) in the 2020 United States Geological Survey (USGS) national seismic hazard maps.

Considering the limitations of amplification database produced through large-scale one-dimensional (1D) site response analyses and simulation-based amplification relationships in HEA19, Ilhan (2020), denoted as I20, suggested new set of amplification dataset with broader coverage of site conditions and improved versions of amplification functions relative to HEA19. Whilst these amplification functions have significantly contributed to the computation of site response at CENA, the underestimation and overestimation of simulated amplification at different site conditions by HEA19 and I20 models are observed from the largely scattered models' residuals that are calculated as the natural logarithm of the ratio of simulated amplification to the estimations of models, albeit the use of complex functional forms in HEA19 and I20. This condition is thought to result from the inherent deficiencies of conventional amplification functions, which fit a priori functional forms to amplification dataset through conventional regression techniques (e.g. linear or nonlinear regression). Thus, Ilhan et al. (2019) utilized deep learning/Artificial Neural Network (ANN) methodology to produce ANN-based models directly learning from dataset without requiring any complex mathematical forms and highlights the noteworthy decrease in the root-mean-square (RMS) error estimations along with the better representation of the amplification at shallow sites (i.e., the sites with depth-to-bedrock ≤ 30 m) relative to conventional relationships of HEA19.

This study further develops the work of Ilhan et al. (2019) to (i) update the structure of ANN-based models to increase the number of outputs from the RS amplification estimations at 22 oscillator periods (T_{OSC}) to those at 115 T_{OSC} values, and (ii) train the ANNs through enhanced and enlarged database of I20 as compared to

HEA19 used in Ilhan et al. (2019). As a result, similar level of reductions in RMS-error attained in Ilhan et al. (2019) are observed, and the improvements by ANNs in capturing site amplification over their conventional counterparts are preserved. Moreover, the ANN and traditional models are further evaluated through their application to a site in New York City to illustrate that the latter can perform slightly better in the representation of the features of peak amplification (e.g., its amplitude and location) and can more accurately capture the period elongation behaviour that stems from the softening of the site profile during nonlinear analyses with high intensity motions relative to conventional relationships.

2 PARAMETRIC STUDY OF 1D SITE RESPONSE ANALYSES

A parametric study of 1D site response simulations was conducted in I20 to capture the variability and uncertainty of site conditions at CENA. The parametric study tree was originally proposed by HEA19 to perform over 1.7 million linear (L), equivalent-linear (EL), and nonlinear (NL) simulations and was updated in I20 to produce a database with larger number of site profiles as shown in Figure 1. I20 parametric study design can be described in detail as follows:

1. A total of 247 recorded and synthetic rock outcrop motions from HEA19 is distributed over all site profiles.
2. Ten geology-dependent base-case V_S profiles are used as input to V_S randomization (Toro, 1995). Nine geology-based soil index properties are associated with these base-case profiles to calculate modulus reduction and damping (MRD) curves (Darendeli, 2001).
3. Thirty randomized V_S profiles are generated for each base-case V_S profile.
4. Three realizations of MRD curves from Darendeli (2001) are produced for mean, systematically high (+ε), and low (-ε) conditions.
5. Each randomized profile is truncated at 18 randomly selected depth-to-rock (Z_{Soil}) conditions from 5.0 m to 1000.0 m to account for the depth-dependent amplification.
6. Seven weathered rock zone (WRZ) models are appended at the bottom of each randomized profile to represent the transition from soil horizon to bedrock condition.

This approach results in 148,050 unique randomized (or generic) V_S profiles, leading to 3,656,835 1D site response analyses, each of 1,218,945 L, EL and NL simulations. All the analyses were carried out using DEEPSOIL V7.0 (Hashash et al., 2017) software through high-performance computing (HPC) resources in Stampede2 (Stanzione et al., 2017) of Texas Advanced Computing Center (TACC).

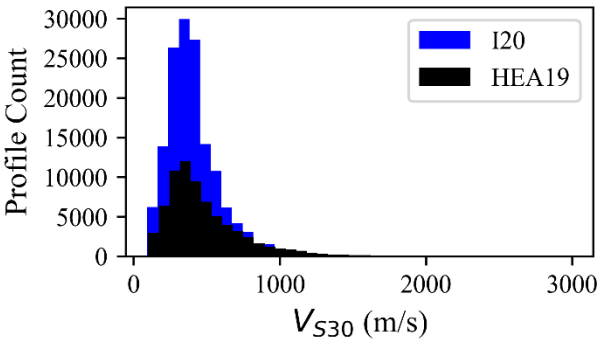

Figure 1. V_{S30} histogram of I20 and HEA19 profiles

3 ANN-BASED SITE AMPLIFICATION MODELS FOR CENA

The total amplification (F_S) without multi-dimensional and basin effects is defined as the natural logarithm of the ratio of the GMIM at the ground surface to the GMIM at the reference condition (V_S = 3000 m/s). It is usually divided into linear (F_{lin}) and nonlinear (F_{nl}) components as given in the Equation (1).

$$F_S = F_{lin} + F_{nl} \quad (1)$$

F_{lin} occurs under relatively weak ground motions and depends on only site properties. F_{nl} term regards the degradation of shear modulus and corresponding damping increase under high-intensity motions and is conditioned on both site and motion properties. The linear and total amplification to train ANNs is obtained from linear-elastic frequency-domain and nonlinear simulations, respectively, from I20.

3.1 Deep learning concept

ANN was devised in McCulloch and Pitts (1943) through mimicking the anatomy of a neuron cell of a human, which is composed of (a) dendrites receiving the input signals, (b) cell body and axon that transmit the signals to (c) terminal axon which outputs signal. Similarly, a neuron in ANN is designed to accept multiple inputs that are processed through a node which is assigned with a function and outputs a value. Then, all the individual neurons are interconnected to create the whole network of ANN. For each neuron, a net and an activation function are defined such that the former combines the inputs to the neuron:

$$Y_j = \sum_{j=1}^{M} w_{ij} \cdot X_i + b_j \quad (2)$$

where w_{ji} is the weight connection of i^{th} input to the j^{th} hidden unit, X_i are inputs, b_j is the bias of the j^{th} unit, Y_j is the output of the Equation (2), and M is the number of data. Activation function introduces nonlinearity in the neural network calculations to solve non-trivial problems that might not easily be dealt with conventional regression models and associates the Y parameter with the output of the neuron as a = *f(Y)*. The commonly

used activation functions are sigmoid, tangent hyperbolic, linear, Rectified Linear Unit (ReLU). These two functions are executed through ANN with interconnected neurons to perform distributed computing.

Table 1. List of ANN and conventional RS and models

ANNs	Conventional	Model Type	Model Parameters
AL1	L1	Linear	V_{S30}
AL5	L5	Linear	V_{S30}, T_{nat}
AT1	L1+N2	Total	V_{S30}, PGA_r
AT5	L5+N2	Total	V_{S30}, T_{nat}, PGA_r

The ANN methodology has begun to be utilized as an alternative to traditional functions in producing ground motion models (GMMs) and amplification functions. Derras et al. (2012) developed an ANN structure including one hidden layer having 20 nodes along with input and output layers to predict peak ground acceleration (PGA) values for KiK-net sites. The database for training the ANN consists of 3891 events from 398 stations with 3.5 ≤ moment magnitude (M_w) ≤ 7.5 and R ≤ 343 km. The independent variables were selected as M_w, the focal depth, R, site resonance frequency, and V_{S30} (the time-averaged V_S in the upper 30 m). The tangent hyperbolic function was preferred as the activation function. ANN-based PGA model was shown to produce lower standard deviation value relative to traditional GMM. Khosravikia et al. (2019) focused on the strong ground motion data from the seismic events occurred in the states of Texas, Oklahoma, and Kansas to suggest ANN-based GMM for the prediction of PGA, PGV (peak ground velocity), and 5% damped spectral accelerations (SA) at 20 periods. Large correlation coefficients (R^2 > 0.8) between the target and predicted values were obtained.

ANN technique has been implemented to capture the simulated and empirical site amplification. Ilhan et al. (2019) trained ANNs using 90% of HEA19 RS and FAS simulated amplification dataset and demonstrated that the reduction in the root-mean-square (RMS) error up to 30% was obtained by ANNs as compared to their conventional counterparts using identical input parameters. Analogously, Roten and Olsen (2021) created convolutional neural network (CNN) using 600 KiK net sites to model the surface-to-borehole Fourier amplification factors (AFs). The velocity profiles of 90% of the sites were inputted to CNN to train the models, and 10% of the sites was determined as testing dataset. The assessment of CNN's performance in representing the observed AFs was conducted through comparison with theoretical SH 1D amplification, resulting in the decrease in prediction error by the former.

Contemplating the definition in the Equation (1) and the improvements by ANNs over traditional relationships, the design of ANNs in this work can be detailed as follows:

- The inputs are (i) only V_{S30} and, V_{S30} and T_{nat} (site natural period), and (ii) V_{S30}, T_{nat} and PGA_r for linear and total RS models, respectively (Table 1).
- The hidden layer includes two layers with 200 nodes.
- The output is RS ln(amplification) at 125 T_{OSC} from 0.001 s to 10.0 s.
- The activation function is selected as ReLU and linear for hidden and output layers, respectively.

The structure of ANN-based model is illustrated in Figure 2. Ninety percent of the data, which correspond to 1,097,050 linear and 999,460 nonlinear analyses, are used to train the models. The remaining 10% of the data is utilized as testing dataset. The loss function for error computation is selected as sum of the square of the differences between simulated data and the estimations. The value of learning rate and the number of epochs is taken as 0.0001 and 5000, respectively.

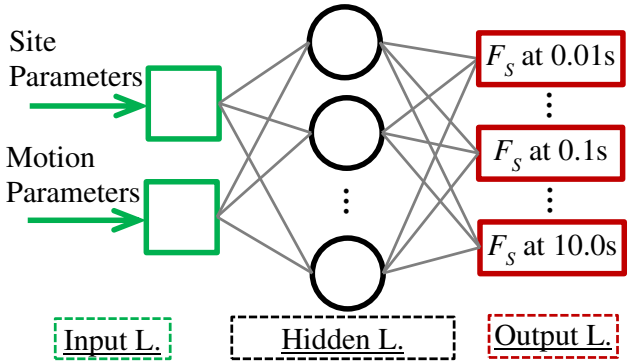

Figure 2. Schematic structure for all ANN-based RS models

The optimization algorithm is determined as Adam optimizer (Kingma and Ba, 2014), which is a stochastic gradient descent method and is proper for training a large amount of data. Tensorflow (Abadi et al., 2016) is used in the Python environment to train the ANNs.

3.2 *ANN vs. conventional models*

The evaluation of how well ANN-based linear RS AL1 and total RS AT1 can predict the simulated amplification is performed through comparisons with their conventional linear L1 and total L1+N2 counterparts, respectively, using identical inputs of ANNs as illustrated in Table 1. These functions can be written as follows:

$$F_{lin} = f(V_{S30}) \mid f(T_{nat}) \quad (3)$$

$$F_S = f(V_{S30}) \mid f(T_{nat}) + f(NL) \quad (4)$$

where $f(V_{S30})$ and $f(T_{nat})$ terms are identical to those in I20. f(NL) represents the nonlinear amplification component analogous to N2 in I20 and HEA19. To emphasize the complexity of these functional forms, the fact that L5 and L5+N2 models possess 10 and 14 different coefficients, respectively, should be declared.

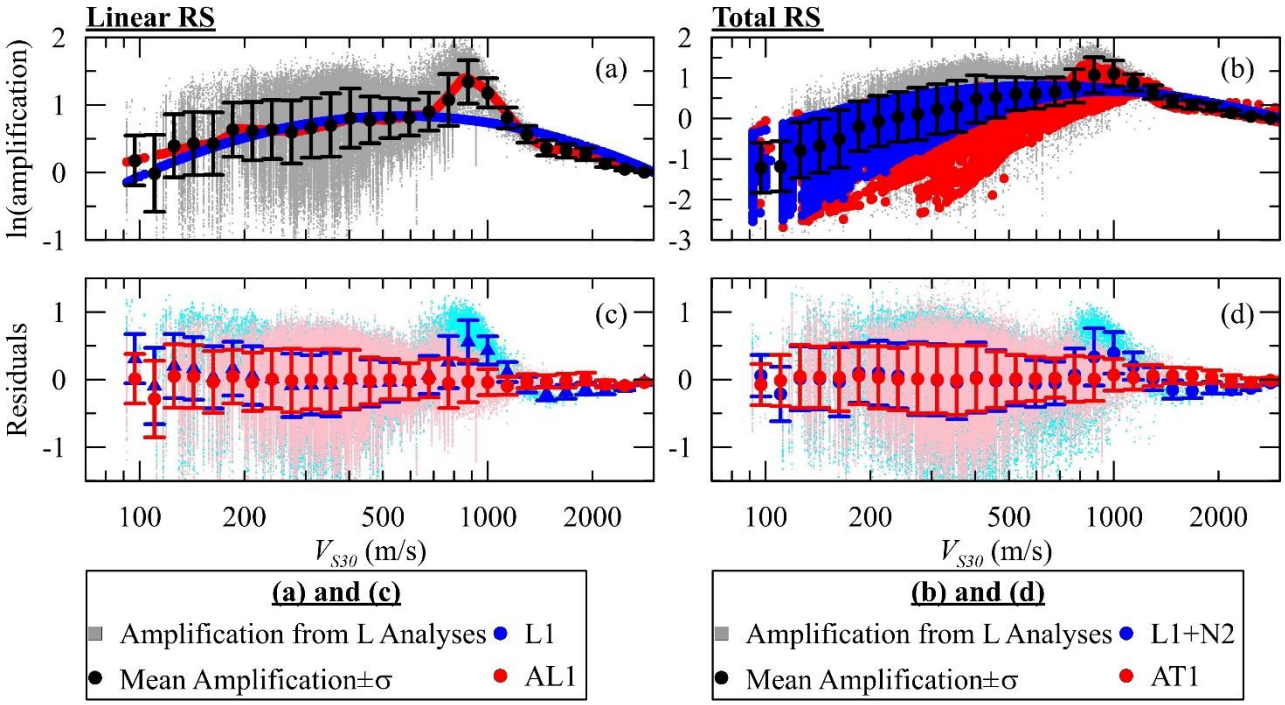

Figure 3. Comparison of estimations and residuals from linear RS (a, c) AL1 and L1 models, and total RS (b, d) AT1 and L1+N2 models for T_{OSC} of 0.1 s. The simulated linear RS ln(amplification) from linear analyses and total RS ln(amplification) from nonlinear analyses along with their mean ±1σ are also presented (Testing dataset).

Figure 3 exhibits the linear RS AL1 and L1, and total RS AT1 and L1+N2 model estimations along with the testing simulated amplification dataset for T_{OSC} of 0.1s. The residuals of ANN-based and conventional models in Figure 3 are calculated as the natural logarithm of the ratio of simulated amplification to models' estimations. The averaged residuals of L1 (Figure 3(c) and Figure 3(d)) as a function of V_{S30} exhibit observable deviations from zero line for $V_{S30} \leq 150$ m/s, and 700 m/s $\leq V_{S30} \leq$ 1100 m/s. Similar offset of L1+N2' residuals from zero is seen for 700 m/s $\leq V_{S30} \leq$ 1100 m/s. This observation highlights that L1 and L1+N2 models cannot capture the complicated nature of the large-scale simulated amplification dataset, albeit possessing complex mathematical forms. However, AL1 can more accurately capture the linear RS data (e.g. the peak at V_{S30} ~ 900 m/s in Figure 3(a)), and the averaged residuals of AL1 (Figure 3(c)) and AT1 (Figure 3(d)) are fully aligned with zero. Additionally, the scatter of ANNs' residuals is observably less than L1 and L1+N2, indicating that the data-driven approach (i.e., deep learning method) seem to be better alternative as compared to conventional techniques in representing large-size databases.

3.3 Models' residual analysis

The alternative performance assessment of conventional models and ANNs is carried out through the standard deviation (σ) of the models' residuals, which is obtained as given in the Equation (5).

$$Residuals = ln\left(\frac{Simulated\ Amplification}{Model\ Estimations}\right) \quad (5)$$

Figure 4 presents the σ of the residuals of conventional linear L1, L5 and total L5+N2, and ANN-based linear AL1, AL5 and total AT5 RS amplification models computed using training dataset. Even though the reduction in the σ of the residuals of AL1 is limited as compared to L1 (e.g., only up to 6.9%), such decrease becomes more explicit in σ of the residuals of AL5 and AT5 that are less than those of traditional L5 and L5+N2 up to 21.5% and 25.1%. This outcome highlights the merit in employing for deep learning-based techniques in modeling site amplification as a substitute of traditional regression methodologies.

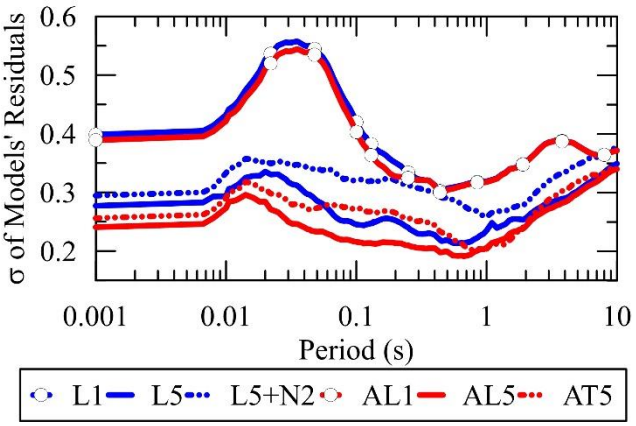

Figure 4. Comparison of standard deviation (σ) of L1, L5, L5+N2, AL1, AL5, and AT5 models' residuals.

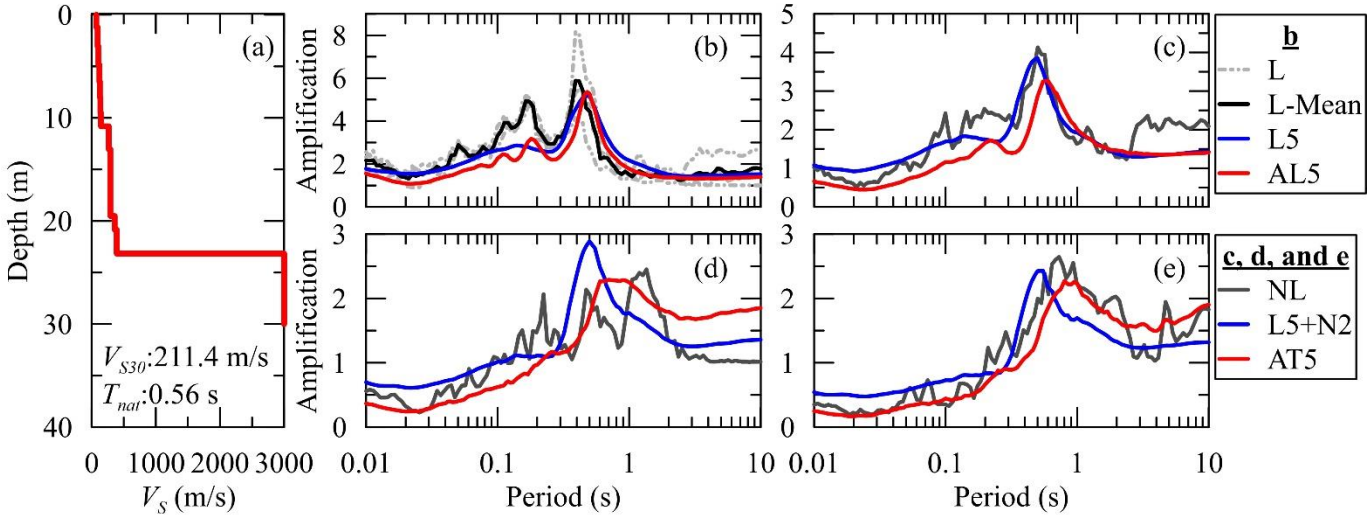

Figure 5. (a) V_S profile of NYC site, (b) comparison of linear RS L5 and AL5 estimations and linear RS amplification data from 3 motions along with its mean, and comparison of estimations from total RS L5+N2 and AT5 and amplification from NL analysis for motions with PGA_r of (c) 0.1 g, (d) 0.3 g, and (e) 0.51 g.

4 SITE-SPECIFIC PERFORMANCE OF AMPLIFICATION MODELS

This section is allocated for the performance evaluation of conventional functions and ANNs in modeling the simulated site-specific response of a profile in New York City (NYC), which are quantified by a suite of 1D NL and L analyses. For these 1D simulations:

- Three rock outcrop motions with PGA of 0.1g, 0.3g and 0.51g are selected from HEA19.
- The V_S profile is presented in Figure 5(a), and V_S of bedrock is taken as 3000 m/s (Hashash et al., 2014).
- The stratigraphy of NYC site (site 15 in Nikolaou et al., 2001) is composed of (i) a highly-plastic organic clay material (OH) from ground surface to 10.0 m, (ii) a poorly graded silty sand soil (SP-SM) with thickness of 13.7 m underlying the OH horizon.
- The reference MRD curves are produced using Darendeli (2001), and General Quadratic and Hyperbolic model (Groholski et al., 2016) is fit to reference curves to consider the shear strength as a limiting stress at large strains (10%).

Figure 5(b) exhibits the site-specific linear RS amplification from three motions along their mean, and AL5 and L5 estimations. The strong impedance between the soil material and the underlying hard-rock condition leads to the distant peak amplification around T_{OSC} ~ 0.45 s (Figure 5(b)). The level of the peak is acceptably captured by both median L5 and AL5, but the latter can fairly represent the location of the 2nd mode amplification around T_{OSC} ~ 0.18 s, which cannot be produced by L5.

The benefit of using ANN is more explicit in comparison between AT5 and L5+N2 for total amplification from NL simulations (Figure 5(c)-(e)). The location of 1st mode peak seems to occur at $T_{OSC} \approx$ 0.5 s for analyses with motion of 0.1 g to shift to longer periods for analyses with motions of increasing PGA values due to period elongation in nonlinear (NL) analyses. This behaviour cannot be captured by L5+N2 since the peak location is provided as a constant input value of T_{OSC}/T_{nat} = 0.81 to L5+N2, but AT5 seems to better account for this shift due to the ability of deep learning methodology to adjust itself compatible with the features of data.

5 CONCLUSION

This paper presents deep learning/ANN-based linear RS and total RS site amplification models trained using simulated amplification obtained from large-scale 1D site response simulations (over 3.6 million L+EL+NL analyses) of site conditions at CENA. ANNs are shown to better represent the amplification dataset relative to amplification functions regressed using conventional techniques such that ANNs reduce the standard deviation of the residuals of linear and total amplification estimations up to 21.5% and 25.1% relative to their conventional counterparts. The ANNs can account for the features of site-specific linear RS amplification (e.g., the location and amplitude of 1st mode peak) as similar to conventional functions and can further represent the 2nd-order peak observed in the simulated amplification. Furthermore, the shift in the location of peak total amplification that stems from the period elongation behavior due to softening of the profile during NL analyses and cannot be captured by conventional models can be fairly modeled by ANNs.

This study highlights that data-driven approaches might be a better alternative for modeling large-scale data as compared to traditional functions forcing predetermined mathematical forms to fit the dataset. However, ANNs cannot be used to predict the

amplification at the site and motion combinations outside of the training space. Therefore, conventional models might be adopted for such situations.

6 ACKNOWLEDGEMENTS

The authors would like to thank Jonathan P. Stewart of University of California, Los Angeles, Ellen M. Rathje of University of Texas at Austin, Sissy Nikolaou of National Institute of Standards and Technology, and Kenneth W. Campbell of CoreLogic for their significant contributions to this study.

7 REFERENCES

Abadi, M., Barham, P., Chen, J., Chen, Z., Davis, A., Dean, J., Devin, M., Ghemawat, S., Irving, G., Isard, M., Kudlur, M., Levenberg, J., Monga, R., …, Tucker, P. et. al. 2016. Tensorflow: A system for large-scale machine learning. *In 12th {USENIX} Symposium on Operating Systems Design and Implementation* ({OSDI} 16) (265-283).

Building Seismic Safety Council (BSSC) 2015. NEHRP Recommended Seismic Provisions for New Buildings and Other Structures **Volume 1**: Part 1 Provisions, Part 2 Commentary, FEMA P-1050-1 Washington, D.C. 555 pp

Darendeli, M. B. 2001. Development of a new family of normalized modulus reduction and material damping curves Ph. D., University of Texas at Austin.

Derras, B., Bard, P. Y., Cotton, F., Bekkouche, A. 2012 Adapting the neural network approach to PGA prediction: An example based on the KiK-net data. *Bulletin of the Seismological Society of America* **102(4)**, 1446-1461.

Frankel, A. D., Mueller, C., Barnhard, T., Perkins, D., Leyendecker, E., Dickman, N., Hanson, S, Hopper, M. 1996. National seismic-hazard maps: documentation June 1996 (96-532). Reston, VA: US Geological Survey.

Groholski, D. R., Hashash, Y. M., Kim, B., Musgrove, M., Harmon, J., Stewart, J. P. 2016. Simplified model for small-strain nonlinearity and strength in 1D seismic site response analysis. *Journal of Geotechnical and Geoenvironmental Engineering* **142(9)**, 04016042.

Harmon, J., Hashash, Y. M., Stewart, J. P., Rathje, E. M., Campbell, K. W., Silva, W. J., Xu, B., Musgrove, M. I, Ilhan, O. 2019. Site amplification functions for central and eastern North America–Part I: Simulation data set development. *Earthquake Spectra* **35(2)**, 787-814.

Harmon, J., Hashash, Y. M., Stewart, J. P., Rathje, E. M., Campbell, K. W., Silva, W. J., Ilhan, O. 2019. Site amplification functions for central and eastern North America–Part II: Modular simulation-based models. *Earthquake Spectra* **35(2)**, 815-847.

Hashash, Y. M. A., Kottke. A. R., Stewart. J. P., Campbell, K. W., Kim, B., Moss, C., Nikolaou, S., Rathje, E. M., Silva, W. J. 2014. Reference Rock Site Condition for Central and Eastern North America. *Bulletin of the Seismological Society of America* **104(2)**: 684-701

Hashash, Y. M., Ilhan, O., Harmon, J. A., Parker, G. A., Stewart, J. P., Rathje, E. M., Campbell, K. W, Silva, W. J. 2020. Nonlinear site amplification model for ergodic seismic hazard analysis in central and eastern North America. *Earthquake Spectra* **36(1)**, 69-86.

Hashash, Y. M. A., Musgrove, M. I., Harmon, J. A., Ilhan, O., Xing, G., Numanoglu, O., Groholski, D.R., Phillips, C.A., Park, D. 2020. DEEPSOIL V7. 0, User Manual, Board of Trustees of University of Illinois at Urbana-Champaign. Urbana, Illinois, USA.

Ilhan, O. (2020). Conventional and deep learning-based site amplification models for central and eastern North America (Doctoral dissertation, University of Illinois at Urbana-Champaign).

Ilhan, O., Harmon, J. A., Numanoglu, O. A., Hashash, Y. M. 2019. Deep learning-based site amplification models for Central and Eastern North America. *In Earthquake Geotechnical Engineering for Protection and Development of Environment and Constructions* (2980-2987).

Khosravikia, F., Clayton, P., Nagy, Z. 2019. Artificial neural network-based framework for developing ground-motion models for natural and induced earthquakes in Oklahoma, Kansas, and Texas. *Seismological Research Letters* **90(2A)**, 604-613.

Kingma, D. P., and Ba, J. 2014. Adam: A method for stochastic optimization. arXiv preprint arXiv:1412.6980.

McCulloch, W. S., Pitts, W. 1943. A logical calculus of the ideas immanent in nervous activity. *The bulletin of mathematical biophysics* **5(4)**, 115-133.

Nikolaou, S., Mylonakis, G., Edinger, P. 2001. Evaluation of site factors for seismic bridge design in New York City area. *Journal of Bridge Engineering* **6(6)**, 564-576.

Parker, G. A., Stewart, J. P., Hashash, Y. M., Rathje, E. M., Campbell, K. W., Silva, W. J. 2019 Empirical linear seismic site amplification in central and eastern North America. *Earthquake Spectra* **35(2)**, 849-881.

Roten, D., Olsen, K. B. 2021. Estimation of site amplification from geotechnical array data using neural networks. *Bulletin of the Seismological Society of America* **111(4)**, 1784-1794.

Seed, H. B., Romo, M. P., Sun, J. I., Jaime, A., Lysmer, J. 1988. The Mexico earthquake of September 19, 1985—Relationships between soil conditions and earthquake ground motions. *Earthquake spectra* **4(4)**, 687-729.

Seyhan, E., Stewart, J. P. 2014. Semi-empirical nonlinear site amplification from NGA-West2 data and simulations. *Earthquake Spectra* **30(3)**, 1241-1256.

Stanzione, D., Barth, B., Gaffney, N., Gaither, K., Hempel, C., Minyard, T., Mehringer, S., Wernert, E., Tufo, H., Panda, D., Teller, P. 2017 Stampede 2: The evolution of an xsede supercomputer. In Proc. of the Practice and Experience in Advanced Research Comp. 2017 on Sustainability, Success and Impact (1-8).

Stewart, J. P., Parker, G. A., Atkinson, G. M., Boore, D. M., Hashash, Y. M., Silva, W. J. 2020. Ergodic site amplification model for central and eastern North America. *Earthquake Spectra* **36(1)**, 42-68.

Toro, G. R. 1995. Probabilistic models of site velocity profiles for generic and site-specific ground-motion amplification studies. Upton, New York, Brookhaven National Laboratory.